

The Pennsylvania State University

The Graduate School

Department of Meteorology

ENSO INFLUENCE ON TROPICAL CYCLONE REGIONAL LANDFALL COUNTS

A Thesis in

Meteorology

by

Kyle Imhoff

© 2014 Kyle Imhoff

Submitted in Partial Fulfillment
of the Requirements
for the Degree of

Master of Science

August 2014

The thesis of Kyle Imhoff was reviewed and approved* by the following:

George S. Young
Professor of Meteorology
Thesis Advisor

Steven Feldstein
Professor of Meteorology

Steven Greybush
Professor of Meteorology

Paul G. Knight
Senior Lecturer in Meteorology
Pennsylvania State Climatologist

Johannes Verlinde
Professor of Meteorology
Associate Head, Graduate Program in Meteorology

*Signatures are on file in the Graduate School

ABSTRACT

A climatological analysis investigates Atlantic basin tropical cyclone tracks and landfall patterns and their connections to synoptic patterns and the phase of the El Niño-Southern Oscillation (ENSO). Thirty-three years (1979-2011) of tropical cyclone activity are examined using storm positions from the North Atlantic Hurricane Database. The ENSO phase is determined by the Oceanic Niño Index, and mean sea level pressure (MSLP) patterns are analyzed using the National Center for Environmental Prediction Reanalysis 2 dataset. A cluster analysis technique, called self-organizing maps, is performed on the MSLP patterns across the North Atlantic Basin at the time when tropical cyclones made landfall. From this technique, statistical comparisons are made between landfall patterns during each ENSO phase and a computed climatological average for each cluster.

Results of this analysis indicate that two distinct high pressure centers are present during La Niña events – one center over the subtropical Atlantic and one over the central United States (US). Only one large high pressure center is present over the Atlantic during El Niño events. Because of these pressure patterns, during La Niña events when more tropical cyclones are favored to form over the Atlantic Basin, greater increases in landfall probabilities exist for Canada and Central America than in the US. During El Niño events when tropical cyclones are less likely to form, smaller decreases in landfall probabilities exist for the US than for Canada and Central America. Thus, landfall activity in the US is less influenced by the ENSO phase than the remainder of the continent.

TABLE OF CONTENTS

List of Figures	v
List of Tables	vi
Acknowledgements.....	vii
Preface.. ..	viii
Chapter 1 Introduction	1
Chapter 2 Methods.....	3
Data	3
Analysis.....	4
Chapter 3 Results	6
Correlations of ENSO with seasonal TC counts	6
Influences of ENSO on MSLP patterns	7
Chapter 4 Conclusions	21
References.....	24

LIST OF FIGURES

Figure 3-1a. Neurons 1 and 2 of the self-organizing map. Each neuron represents the average mean sea-level pressure pattern in each cluster. Shading indicates mean sea level pressure measured in Pascals. Tracks of storms (in white) within each neuron are overlaid on the pressure patterns. Blue dots indicate landfalls during La Nina months and red dots indicate landfalls during El Nino months.	9
Figure 3-1b. Same as in Fig. 3-1a except neurons 3 and 4.	10
Figure 3-1c. Same as in Fig. 3-1a except neurons 5 and 6.	11
Figure 3-1d. Same as in Fig. 3-1a except neurons 7 and 8.	12
Figure 3-2. Maps of all landfalls along the main coastline of North America. The left map shows all landfalls of tropical cyclones during El Nino months (in red) and La Nina months (in blue). The right map shows all landfalls during neutral months.	20

LIST OF TABLES

- Table 3-1. Linear regression analysis that quantifies the statistical significance of how closely responses of given tropical cyclone track/landfall patterns to the phase of ENSO resemble linearity. “Total” categories include both landfalling and non-landfalling tropical cyclones.7
- Table 3-2. A comparison of tropical cyclone landfall counts for each ENSO phase over all tropical cyclone region/ocean categorizations included in this study to each neuron’s climatological average number of tropical cyclones – these can be thought of as anomalies from each neuron’s climatological average. The storm count column shows the total number of storms as well as the number that landfall in each ENSO phase for each neuron. Decimals in the tables below represent fractions of number of storms in each neuron and category out of the total in each ENSO phase. So, for example, the “US Atlantic” category in the “El Nino” row for neuron 1 would be equal to: (number of storms that formed in the Atlantic that hit the US during an El Nino month in neuron 1/total number of El Nino landfall storms over the 33 year period) – Climo row (total number of storms that formed in the Atlantic that hit the US during both El Nino and La Nina months in Neuron 1/total number of storms in hurricane seasons over the 33 year period).14

ACKNOWLEDGEMENTS

The authors would like to thank the review of this work and the valuable insights provided by Dr. George Young, Dr. Steven Feldstein, Paul Knight, and Dr. Steven Greybush. Dr. Jenni Evans provided beneficial guidance with respect to methodologies in analyzing tropical cyclone tracks. The authors are also very grateful to the following organizations for providing data that made this investigation possible: National Centers for Environmental Prediction, National Center for Atmospheric Research, NOAA Earth System Research Laboratory, and the NOAA Hurricane Research Division.

PREFACE

The following thesis was written with the intention of submission to the Journal of Operational Meteorology in collaboration with advisor and co-author Dr. George Young. All of the writing and primary research work was completed by the first author of the article and the author of this thesis, Kyle Imhoff. Dr. Young provided guidance and scientific insight to the investigation in addition to edits to the paper which supported a co-authorship title on the paper.

Chapter 1

Introduction

Tropical cyclones in the Atlantic basin have a large socioeconomic impact on inhabitants along the eastern coast of North America (Pielke and Pielke 1997). Over the past few decades, people have increasingly re-located to, and have built property in, coastal regions (known as “coastal migration”), which has increased the potential impacts of these storms (Pielke and Landsea 1998). Because of the extensive losses associated with these storms, considerable research has been performed over the past few decades to develop methods by which to accurately predict these storms on a broad range of time scales (e.g., Gray et al. 1993; Gray et al. 1994; Lehmiller et al. 1997; Klotzbach 2014). Of interest here is the ability to predict the severity of a hurricane season, often quantified using the number of named storms, months in advance. This procedure is known as seasonal forecasting.

Seasonal forecasts of tropical cyclone activity in the Atlantic basin, as well as the environmental factors which influence these numbers, have been steadily refined over the past few decades (e.g., Gray 1984b; Gray et al. 1992; Landsea et al. 1994; Hess et al. 1995; Klotzbach and Gray 2008). The El Niño-Southern Oscillation (ENSO) has a relatively large influence on seasonal hurricane activity, with El Niño (positive ENSO phase) events inhibiting storm development in the Atlantic basin and La Niña (negative ENSO phase) events enhancing storm development (Gray 1984a; Goldenberg and Shapiro 1996; Bove et al. 1998; Wilson 1999; Elsner and Jagger 2004; Yan 2006; Klotzbach 2011).

In addition to interannual variability in tropical cyclone activity, track variability is an important factor in determining the potential socioeconomic impacts of a particular storm season.

Many studies recently have looked at how hurricane track and landfall variability is influenced by ENSO phase and the background synoptic scale flow, particularly the variations in the persistent subtropical high that is present over the north-central Atlantic Ocean (Elsner 2003; Klotzbach and Gray 2006; Kossin et al. 2010; Klotzbach 2011; Colbert and Soden 2012). These studies provide valuable insight into how hurricane tracks and landfalls are modulated by planetary and synoptic-scale phenomena. The current study is intended to expand on this prior work by examining the regional impacts of both ENSO and synoptic-scale patterns on tropical cyclone activity. Specifically, the focus of the study is on how these large-scale phenomena influence the interannual variability in regional North American landfall numbers.

Chapter 2

Methods

Data

The tropical cyclones investigated are those that occurred in the period 1979 to 2011 in the North Atlantic basin. Storms that formed outside of the hurricane season date range of 1 June through 30 November were excluded from this analysis to ensure for climatological consistency. Track information and storm strength is determined using the National Hurricane Center's hurricane dataset, HURDAT (available online at http://www.aoml.noaa.gov/hrd/hurdat/tracks1851to2011_atl_reanal.html). Landfall times used for statistical analyses are determined by using either the time associated with a HURDAT position fix along the coastline or the closest HURDAT time prior to landfall in cases where the storm crossed the coast between fixes. Each tropical cyclone is classified as being of Atlantic or Gulf of Mexico (Gulf) origin based on the location at which it became a tropical depression according to HURDAT. Gulf storms were those that formed in the Gulf of Mexico defined as a box bounded by 10 and 30 degrees north latitude and 70 and 100 degrees west longitude; storms outside of this box were classified as Atlantic. Tropical cyclone landfall classifications were separated into three regions based on political boundaries: Canada, United States (US), and Central America.

ENSO phase values are determined using the Oceanic Nino Index (ONI) which is derived from observations of sea surface temperatures in the Nino 3.4 region (available online at: http://www.cpc.ncep.noaa.gov/products/analysis_monitoring/ensostuff/ensoyears.shtml).

Monthly values are estimated from the 3-month running mean values of the ONI. For example, the July-August-September ONI value would be assigned as the August ONI value. Seasonally-averaged ONI values used in the linear regression analysis described in the next section are computed as the mean of the monthly values comprising the hurricane season, June through November. This is done for each year in the period of the study. Months were classified as La Nina when the monthly ONI value was less than 0.5. Conversely, months were classified as El Nino when the monthly ONI value was greater than 0.5. Those with monthly ONI values between these two thresholds were classified as neutral.

Mean sea level pressure patterns used to describe synoptic-scale weather patterns in this study are determined using the National Centers for Environmental Prediction – National Center for Atmospheric Research (NCEP-NCAR) Reanalysis 2 global dataset provided by the NOAA/OAR/ESRL Physical Sciences Division (PSD), Boulder, Colorado, USA (available online at <http://www.esrl.noaa.gov/psd/data/gridded/data.ncep.reanalysis2.html>) that has a horizontal resolution of 2.5 degrees longitude x 2.5 degrees latitude, contains 17 pressure levels in the vertical, and provides data back to 1979 (Kanamitsu et al. 2002).

Analysis

Linear regression analysis was used to determine the responses in seasonal hurricane track characteristics/landfall patterns to seasonally-averaged values of ONI. For this study, the predictor is the seasonally-averaged ONI values and the predictand is the seasonal counts of tropical cyclones in each category described in the next section. Values computed in the analysis were the slope and Y-intercept coefficients of the regression equation $tc_count = m * ONI + b$, the R^2 value, the F-statistic, the P-value, and the standard error of the regression.

A cluster analysis, using Teuvo Kohonen's self-organizing maps (SOM) technique, was performed for mean sea level pressure patterns at the time when tropical cyclones made landfall (Kohonen 2001). To determine the effects of the phase of ENSO (either El Nino or La Nina) on tropical cyclone landfall patterns, neutral storms were excluded from the cluster analysis. Because it is a cluster analysis technique, SOM does not require supervised training, i.e., cases need not be assigned a priori to clusters. Rather the algorithm assigns each case to a cluster (neuron) based on its similarity to the cluster mean (i.e., weight vector). The assignment of cases to neurons involves a competitive process called vector quantization (Kaski 1997). The advantage to using SOM analysis is that high-dimensional data can be reduced down to two-dimensional visualizations, called maps, that aid in human interpretation of the resulting neurons. These neurons have the same spatial domains and units as the input (each individual case), thus they are composite images of the mean sea level pressure patterns illustrating the predominant synoptic regimes in the region. In this study, the SOM analysis is performed using the MATLAB package SOM Toolbox 2.0 (available online at <http://www.cis.hut.fi/projects/somtoolbox/>).

SOMs are produced for mean sea-level pressure patterns at the times at which all tropical cyclones in the period of the study made landfall. The map that is created for each variable is comprised of eight clusters, i.e., archetypical synoptic patterns. In SOM nomenclature these archetypical synoptic patterns are called neurons. The SOM network used in this study consisted of eight neurons in a four-by-two array. This network structure, was selected because it resulted in each neuron having enough tropical cyclones to get a reasonable composite of height/pressure patterns, while still producing distinct patterns in each neuron. Larger domains yielded some neurons with few cases while smaller maps merged synoptic patterns that were rather distinct on the four-by-two array.

Chapter 3

Results

Correlations of ENSO with seasonal TC counts

Linear regression is used to quantify the influence of ENSO on tropical cyclone and landfall counts in the North Atlantic basin and North America. Storms originating in the Atlantic and Gulf of Mexico are considered separately as well as together. The resulting statistics are shown in Table 3-1.

This analysis reveals statistically significant (low P-value) ENSO relationships for a number of the counts. Tropical cyclone counts that include the total number of landfalling storms ('Total Landfall' in Table 3-1) and the total of both landfall and non-landfalling storms ('Total cyclones' in Table 3-1) yield P-values less than 0.01. The R^2 values are moderate (0.20 to 0.26), indicating that ENSO explains a useful fraction of the season-to-season variance in the number of tropical cyclones, and the total number of landfalling storms in North America, in the North Atlantic. El Nino (positive ONI) has a negative influence on storm counts in the Atlantic, Gulf, and total (1 to 3 storms for an ONI difference of 1). These results are in line with numerous previous studies that have shown influences of the phase of ENSO with interannual tropical cyclone count variability (e.g., Gray 1984a; Goldenberg and Shapiro 1996; Wilson 1999).

Regression analysis of the landfall counts on a regional scale paints a more complex picture. Correlations of ENSO with all US landfall count categories (total, Atlantic, and Gulf) fail any reasonable test of statistical significance. In fact, the worst P-value in the study was associated with the correlation of ENSO with US landfalling storms that originate in the Atlantic.

R^2 values are correspondingly small, with 0% to 10% of count variance explained by ONI. A change of 1 unit in ONI causes only a 0.05 to 0.75 change in the number of US landfalls, roughly $\frac{1}{4}$ the impact seen on total storm numbers. This lack of correlation indicates that while El Nino decreases the number of storms in both basins, it correspondingly increases the fraction which make US landfall. The next section describes the use of SOM analysis of archetypical synoptic patterns to determine why El Nino has this counterbalancing impact on US landfall fraction.

Table 3-1. Linear regression analysis that quantifies the statistical significance of how closely responses of given tropical cyclone track/landfall patterns to the phase of ENSO resemble linearity. “Total” categories include both landfalling and non-landfalling tropical cyclones.

Category - ENSO vs. :	Y-Int Coeff	Slope Coeff	R^2 Value	F- statistic	P-value	Error Variance
Total cyclones	11.85	-2.88	0.20	7.70	0.009	4.54
Total Atlantic	7.80	-1.40	0.11	3.67	0.065	3.20
Total Gulf	4.05	-1.48	0.20	7.61	0.010	2.34
Total Landfall	5.34	-2.12	0.26	11.1	0.002	2.78
Total Atlantic Landfall	2.11	-0.68	0.10	3.48	0.072	1.60
Total Gulf Landfall	3.23	-1.44	0.22	8.79	0.006	2.12
Total US Landfall	3.38	-0.74	0.06	2.04	0.164	2.25
Atlantic - US Landfall	1.18	-0.04	0.00	0.02	0.902	1.47
Gulf - US Landfall	2.20	-0.69	0.10	3.57	0.068	1.60
Atlantic – Central America Landfall	0.34	-0.30	0.09	2.99	0.094	0.57
Gulf – Central America Landfall	1.02	-0.74	0.15	5.52	0.025	1.92
Atlantic - Canada Landfall	0.59	-0.35	0.14	5.12	0.031	0.67

Influences of ENSO on MSLP patterns

SOM cluster analysis is used to explore how the phase of ENSO induces changes in the frequency of synoptic scale patterns that affect landfall variability. This analysis is conducted for all three landfall regions, with the largest quantifiable impacts being observed along the US

coastline. Fig. 3-1a-d show the predominant mean sea-level pressure patterns (neurons) at the time of landfall for the tropical cyclones studied that were obtained from the SOM analysis.

Fig. 3-1a-d provide insight into how ENSO affects these synoptic patterns. The neurons in these figures depict variations on two fundamental synoptic patterns. Neurons 1-4 show a single center of high pressure of varying shapes and magnitude located over the subtropical Atlantic. In contrast, neurons 5-8 have two distinct centers of high pressure aligned roughly east-west, separated by a weakness in the pressure field. While seven of the eight neurons in the study had more La Nina landfalls than El Nino landfalls (the exception was neuron 1), all four of the single-anticyclone neurons experienced 33-53% of their landfalls during El Nino months. In contrast, for the double-anticyclone neurons, the overwhelming majority (63-83%) of landfalls occurred during La Nina months.

By separating the neurons of the self-organizing map into these two groups, differences can be seen between the synoptic mean sea-level pressure patterns of landfall days during the two different ENSO phases. Specifically, the characteristics of the subtropical ridge located over the Atlantic are distinctly different between the two ENSO phases. The neurons which contain higher proportions of landfalls during El Nino months, in general, exhibit a stronger subtropical ridge that is larger in areal extent and extends farther to the west/south as compared to that in the predominantly La Nina neurons. The predominantly La Nina neurons contain a much weaker subtropical ridge that is displaced to the north/east compared to neurons with more El Nino landfalls. In addition, for predominantly La Nina neurons, a weakness in the ridge is present between 280-285 degrees longitude that splits the ridge into two centers of high pressure. It should be remembered that these synoptic pattern differences are for times of landfall determined for the storms in this study, not for all days of that ENSO phase.

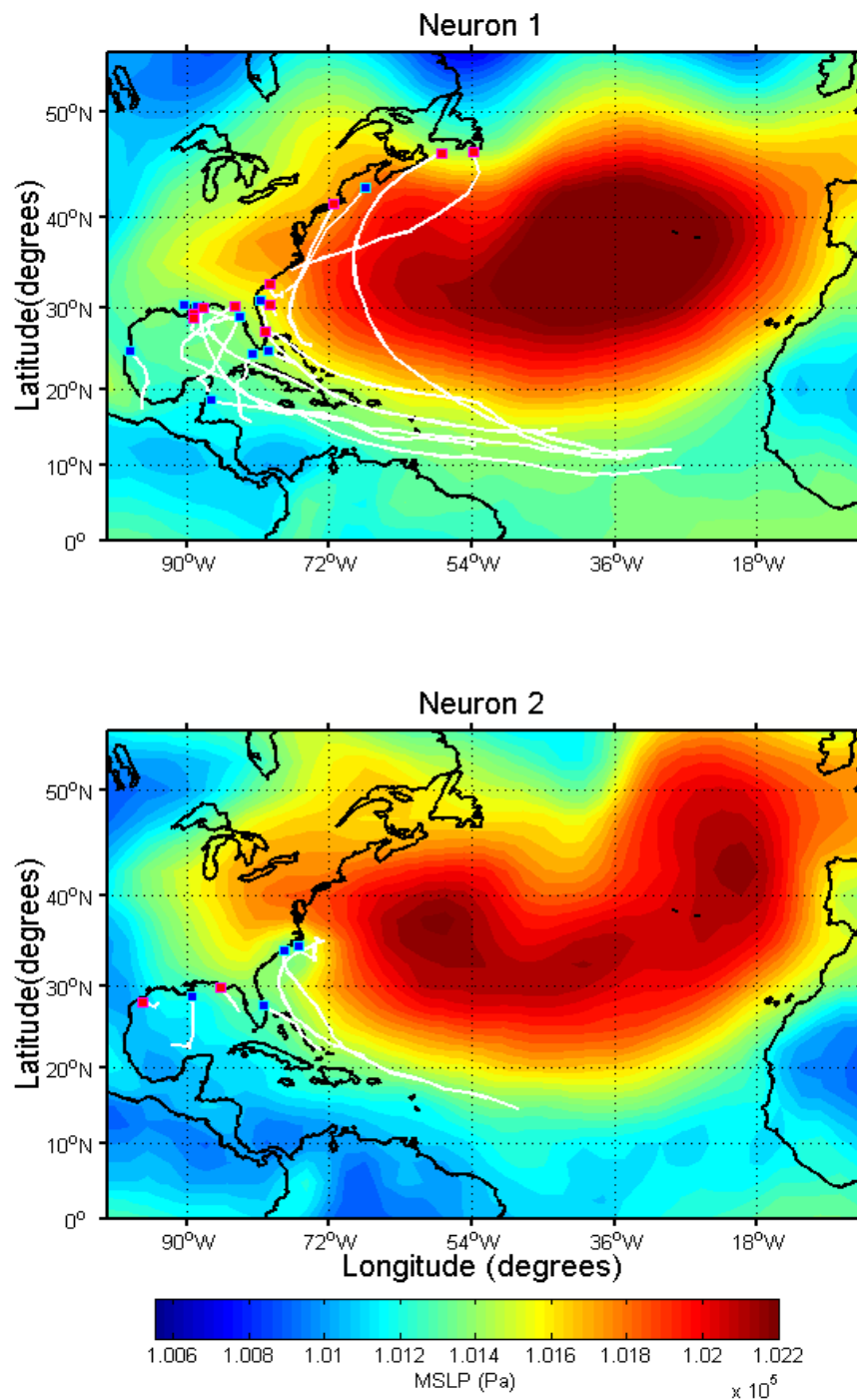


Figure 3-1a. Neurons 1 and 2 of the self-organizing map. Each neuron represents the average mean sea-level pressure pattern in each cluster. Shading indicates mean sea level pressure measured in Pascals. Tracks of storms (in white) within each neuron are overlaid on the pressure patterns. Blue dots indicate landfalls during La Niña months and red dots indicate landfalls during El Niño months.

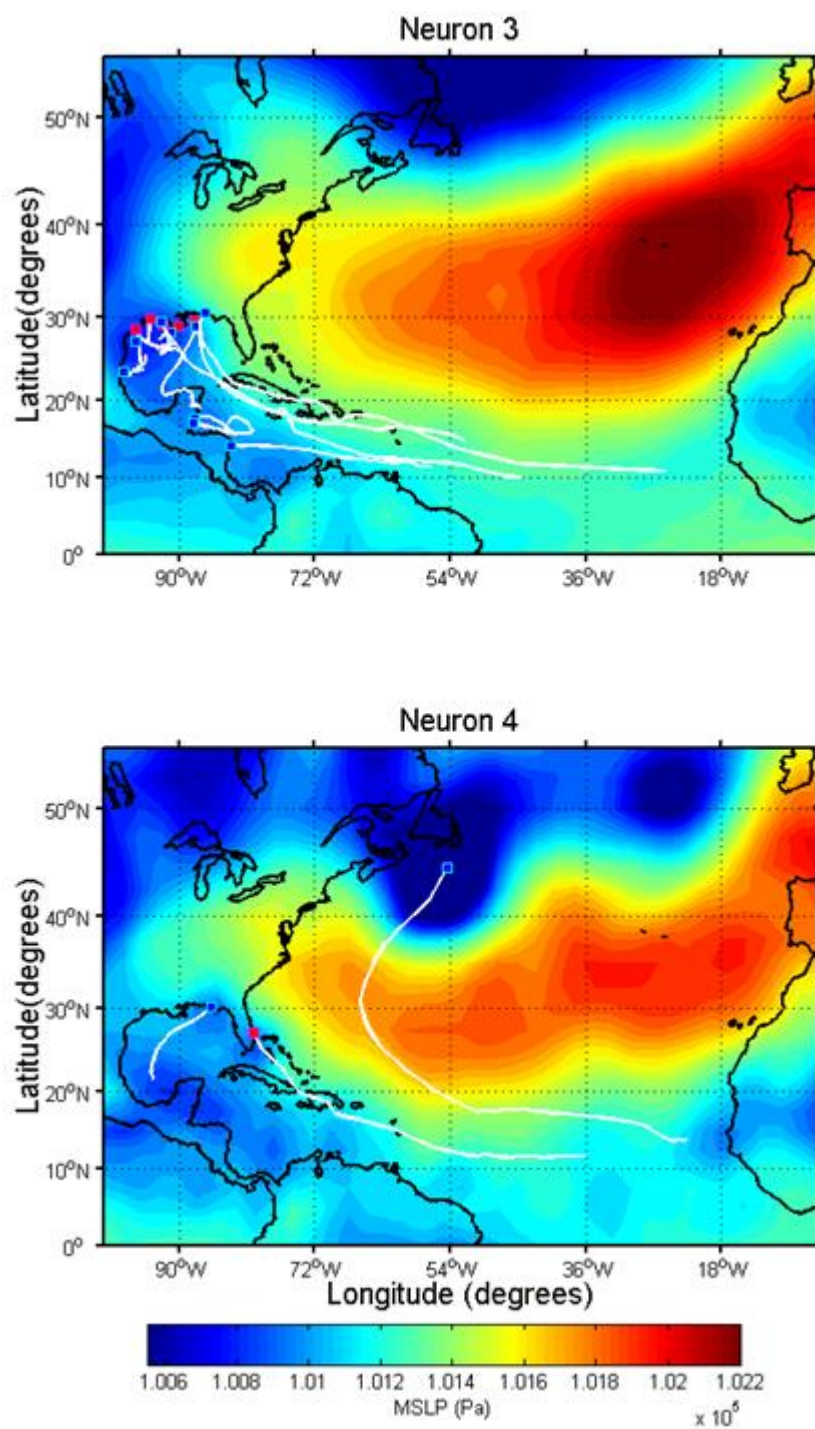


Figure 3-1b. Same as in Fig. 3-1a except neurons 3 and 4.

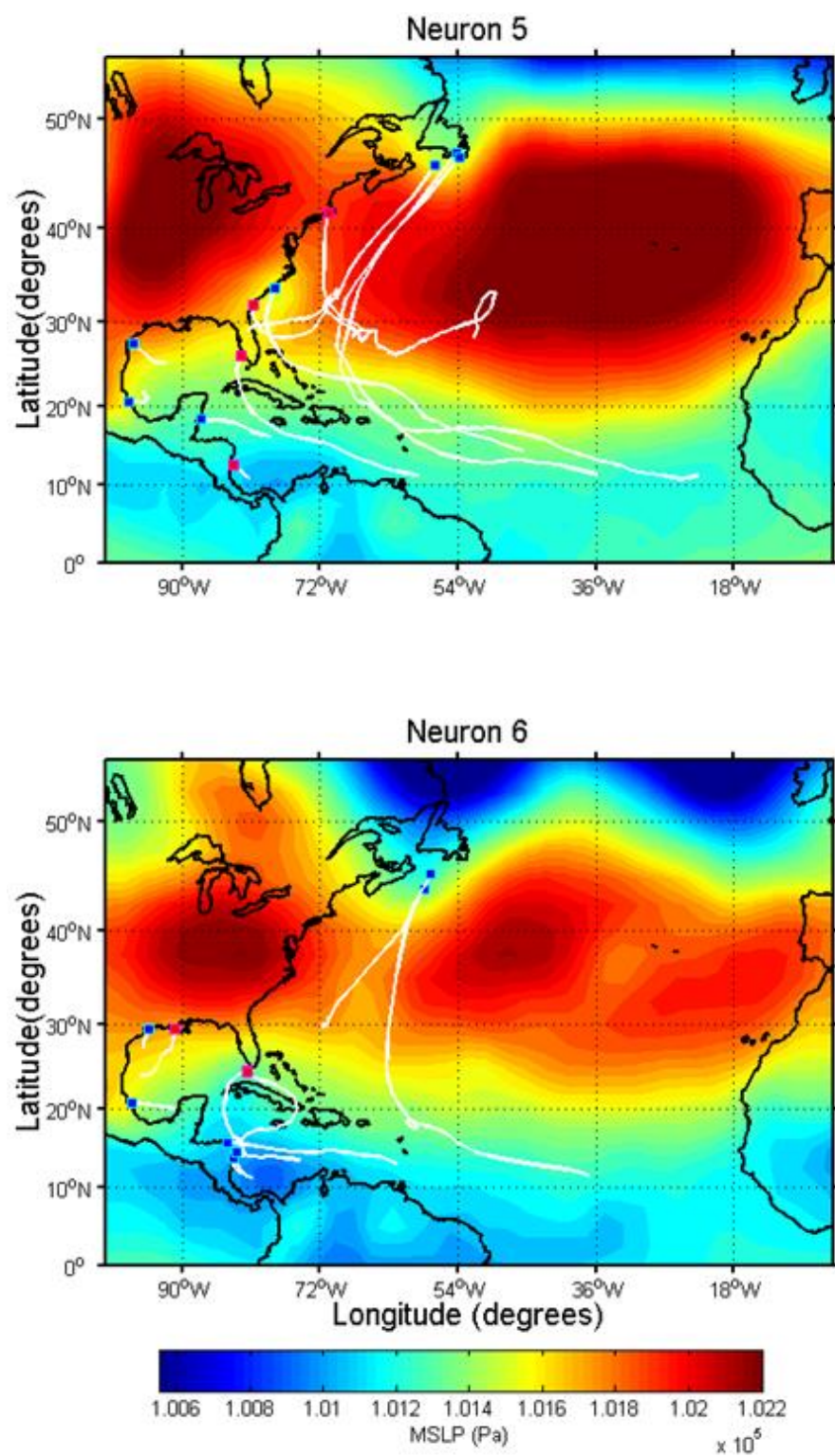


Figure 3-1c. Same as in Fig. 3-1a except neurons 5 and 6.

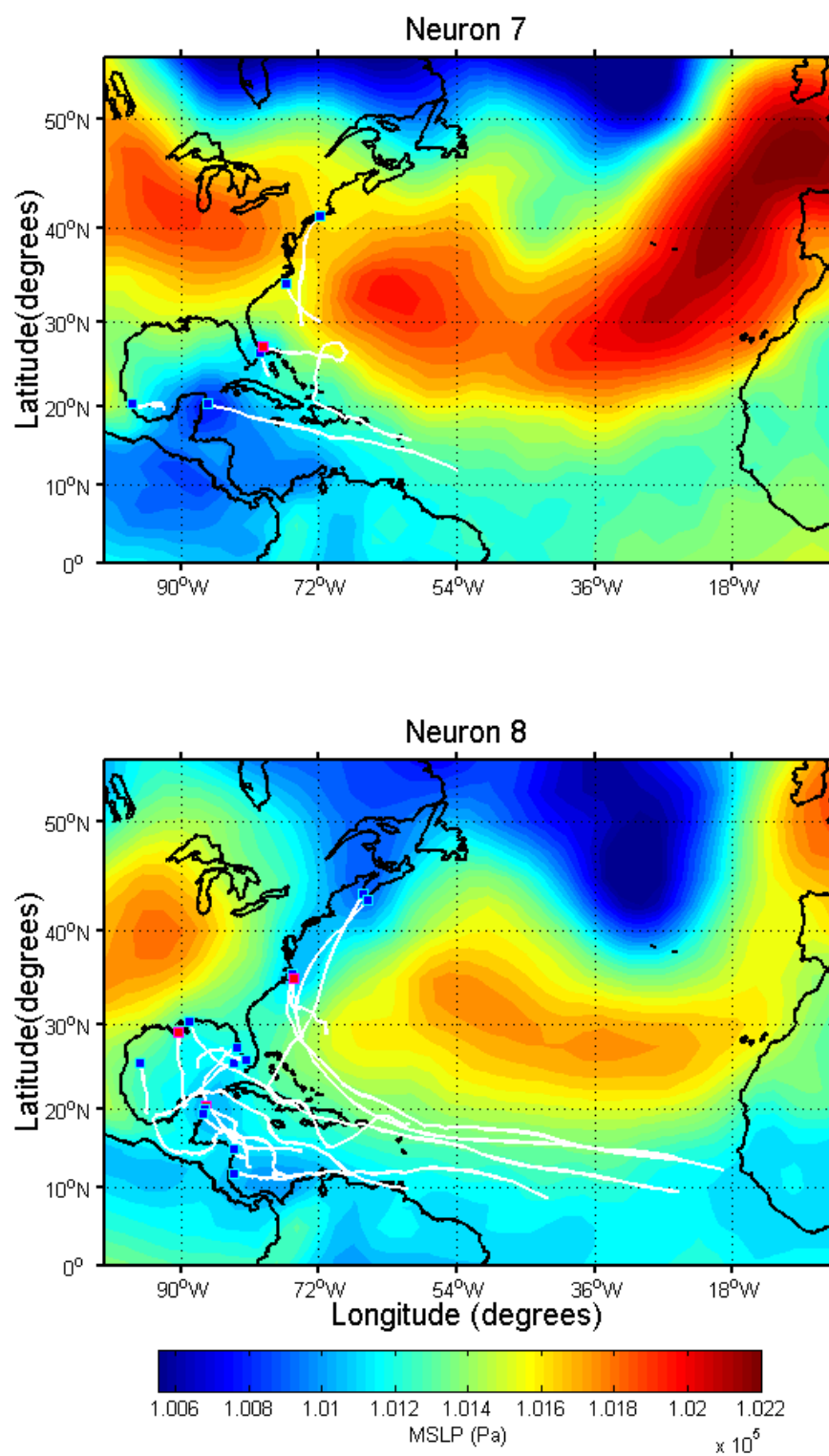


Figure 3-1d. Same as in Fig. 3-1a except neurons 7 and 8.

Previous studies (e.g., Colbert and Soden 2012; Klotzbach 2011) have shown the importance of variations in the subtropical ridge in the tracks of hurricanes in the Atlantic. While our study investigates all tropical cyclones rather than just hurricanes similar advective arguments can be made. These studies have also shown links between the phase of ENSO and the position/strength of the subtropical ridge. Storms that form south of 25 degrees N latitude typically track westward along the southern periphery of the subtropical ridge and begin to recurve poleward at a longitude near the western edge of the ridge where extratropical transition commences (e.g., Hart and Evans 2001; Elsner 2003; Kossin and Vimont 2007; Kossin et. al. 2010). Such storms either miss the mainland of North America or strike the east coast of the US or Canada. This recurvature is inhibited, however, if the ridge's westward edge reaches the east coast of the US. In this synoptic pattern, storms remain farther south throughout their lifecycle, recurve farther westward and, as a result, make landfall along the eastern coast of Central America or enter the Gulf of Mexico and make landfall along the Gulf coast of the US.

Based on this SOM analysis, in particular the characteristics of the subtropical high in each neuron, it can be seen why El Nino conditions favor tracks that threaten the Gulf coast of the US, while La Nina conditions favor tracks that threaten Central America and Canada. The influence of this synoptic pattern on storm tracks provides a potential explanation for findings produced by Klotzbach (2011) in which it was noted that Gulf Coast states had less variability in landfall counts between El Nino/La Nina phase as compared to the east coast of the US. Track plots for storms within each neuron overlaid on the neuron's mean sea-level pressure pattern supports this conclusion (Fig. 3-1a-d).

Table 3-2. A comparison of tropical cyclone landfall counts for each ENSO phase over all tropical cyclone region/ocean categorizations included in this study to each neuron's climatological average number of tropical cyclones – these can be thought of as anomalies from each neuron's climatological average. The storm count column shows the total number of storms as well as the number that landfall in each ENSO phase for each neuron. Decimals in the tables below represent fractions of number of storms in each neuron and category out of the total in each ENSO phase. So, for example, the “US Atlantic” category in the “El Nino” row for neuron 1 would be equal to: (number of storms that formed in the Atlantic that hit the US during an El Nino month in neuron 1/total number of El Nino landfall storms over the 33 year period) – Climo row (total number of storms that formed in the Atlantic that hit the US during both El Nino and La Nina months in Neuron 1/total number of storms in hurricane seasons over the 33 year period).

Neuron	Storm Count		Phase	US Atlantic	US Gulf	Central America Atlantic	Central America Gulf	Canada Atlantic	Total Atlantic	Total Gulf
1	Total	19	Climo	0.060	0.107	0.012	0.012	0.036	0.107	0.119
	El Nino	10	El Nino	0.078	0.031	-0.012	-0.012	0.033	0.100	0.019
	La Nina	9	La Nina	-0.041	-0.016	0.006	0.006	-0.018	-0.053	-0.010
2	Total	6	Climo	0.012	0.060	0.000	0.000	0.000	0.012	0.060
	El Nino	2	El Nino	-0.012	0.009	0.000	0.000	0.000	-0.012	0.009
	La Nina	4	La Nina	0.006	-0.005	0.000	0.000	0.000	0.006	-0.005
3	Total	14	Climo	0.036	0.083	0.012	0.036	0.000	0.048	0.119
	El Nino	5	El Nino	0.033	0.020	-0.012	-0.036	0.000	0.021	-0.016
	La Nina	9	La Nina	-0.018	-0.011	0.006	0.019	0.000	-0.011	0.008
4	Total	3	Climo	0.012	0.012	0.000	0.000	0.012	0.024	0.012
	El Nino	1	El Nino	0.023	-0.012	0.000	0.000	-0.012	0.011	-0.012
	La Nina	2	La Nina	-0.012	0.006	0.000	0.000	0.006	-0.006	0.006
5	Total	11	Climo	0.048	0.012	0.000	0.036	0.024	0.071	0.060
	El Nino	4	El Nino	0.056	-0.012	0.000	-0.001	-0.024	0.032	-0.025
	La Nina	7	La Nina	-0.029	0.006	0.000	0.001	0.013	-0.017	0.013
6	Total	10	Climo	0.000	0.048	0.012	0.036	0.024	0.036	0.083
	El Nino	3	El Nino	0.000	0.056	-0.012	-0.036	-0.024	-0.036	0.020
	La Nina	7	La Nina	0.000	-0.029	0.006	0.019	0.013	0.019	-0.011
7	Total	6	Climo	0.024	0.024	0.012	0.012	0.000	0.036	0.036
	El Nino	1	El Nino	0.011	-0.024	-0.012	-0.012	0.000	-0.001	-0.036
	La Nina	5	La Nina	-0.006	0.013	0.006	0.006	0.000	0.001	0.019
8	Total	15	Climo	0.036	0.060	0.012	0.048	0.024	0.071	0.107
	El Nino	3	El Nino	-0.001	-0.025	-0.012	-0.013	-0.024	-0.037	-0.038
	La Nina	12	La Nina	0.001	0.013	0.006	0.007	0.013	0.019	0.020
Expected Value				0.035	0.062	0.009	0.027	0.019	0.063	0.091

This SOM-based grouping can be exploited to determine which synoptic patterns are responsible for the sensitivity of landfall fraction to ENSO phase. Table 3-2 provides a breakdown of each neuron by ENSO phase, showing the resulting differences in landfall fraction between that phase and the total landfall fraction for that neuron (referred to as *climo* in the table). Comparing the *climo* counts provides information on the contribution of each neuron to the overall landfall statistics. Further, comparing the El Nino and La Nina count anomalies for a neuron quantifies its contribution to the ONI effect described above. For example, a neuron for which the El Nino landfall count anomaly was positive (La Nina landfall count anomaly negative) would contribute to a positive relationship (correlation and slope in Table 3-1) between ONI and regional landfall count.

As mentioned above, storms that make landfall in the US that originate in the Atlantic ('US Atlantic' column in Table 3-2) have the highest P-value associated with the correlation between ONI and seasonal landfall counts. Thus, some of the synoptic patterns captured in the SOM neurons must be producing changes in landfall percentage that counteract the ENSO effect on storm numbers. The synoptic patterns responsible can be determined by examining the counts of El Nino and La Nina storms for each neuron.

The influence of ENSO phase on the predominant synoptic patterns and landfall counts for each neuron and category (e.g., US Atlantic) in Table 3-2 can be separated into two components by using both the climatological values and the landfall count anomalies. The first component is the influence of the neuron as a whole (not accounting for ENSO phase differences). The second component is the effect of ENSO phase interacting with that particular neuron.

The first component can be found by a comparison of the *climo* value (rows labeled '*climo*' in Table 3-2) for each neuron / category pairing to the expected value of that category's landfall fraction per neuron ('Expected value' row in Table 3-2). The expected value of landfalls

for each category is computed in eq. 1, where n is the number of neurons and N is the total number of landfalling storms in the study.

$$E(LF) = \frac{\sum_{i=1}^n (climo_i * total_i)}{N} \quad (1)$$

A neuron whose *climo* value is larger than the expected value indicates a synoptic pattern which favors landfalling storms in that respective category. The opposite holds true for neurons which have *climo* values lower than the expected value for that category.

The impact of this first component on the ENSO signal in landfall numbers can be evaluated by examining the distribution of storms by ENSO phase in each neuron which can then provide insight into whether a synoptic pattern is favored during one phase over the other. So, assessing the first component and the ENSO phase distribution together for each neuron provides insight into the synoptic patterns which favor landfalls in given regions as well as the ENSO phase in which that synoptic pattern is favored. The second component is an examination of the landfall count anomalies for each neuron and each category in Table 3-2. The landfall count anomalies are calculated by subtracting the *climo* value from the fraction of landfalls that occur in each ENSO phase for each neuron. For example, computing the El Nino landfall count anomaly for a given category would be the subtraction of the *climo* value for that neuron / category pairing from the fraction of El Nino landfalls that occur in that neuron out of the total number of El Nino landfalls that occur in the 33-year period of the study. Neurons in which El Nino has a positive landfall count anomaly compared to *climo*, for example, indicates that within a given synoptic pattern landfalls are favored during El Nino months as compared to La Nina months, i.e., the ENSO counter effect. This second component, thus, is a quantification of how the effects of a given neuron's synoptic pattern vary with ENSO phase.

These two components can be used to assess the synoptic patterns which cause landfall counts for the US to respond differently to ENSO phase than do raw tropical storm

numbers for the North Atlantic basin. Neuron 1 is the only neuron to have a majority of storm landfalls during El Nino phase (10 of the 19) and has both strong positive component 1 (i.e., it is responsible for more than its fair share of landfalls) and positive El Nino landfall count anomalies (component 2) for both the US Atlantic and US Gulf categories. Thus, this neuron contributes to the lack of ENSO/count correlation reported in Table 3-1 for these two categories. The shape and size of the subtropical high results in storms tracking along the southern periphery of the ridge and making landfall along the US coastline. Although this is the only neuron to have more El Nino storms form east of 70 degrees West longitude as compared to La Nina storms, those storms that do form farther east are more likely to stay farther south/east initially and then recurve in locations which favor landfall along the US coast (Fig. 3-1a).

Neuron 2 has very few storms (6) with 2/3 of the landfalls occurring during La Nina months. The subtropical high in this neuron is very similar in size and shape to neuron 1 but noticeably weaker. Storm origin locations are farther west than in neuron 1. All six storms make landfall in the US, indicating that the combination of the origin locations and the influence of the subtropical high on storm advection favor landfalls along the US coastline. These influences are relatively independent of ENSO phase, however (no strong component 1 or component 2 anomalies exist from this neuron).

Neuron 3 shows the center of the subtropical high displaced farther to the east as compared to neurons 1 and 2 but still extends west to the east coast of the US. As a result of this, storms preferentially form in the Gulf of Mexico rather than forming out in the central Atlantic, and so make landfall along the adjacent coastlines (Central America and US). This leads to strong positive component 1 for both the US Gulf and Central America Gulf categories. An interesting dichotomy exists between the two phases of ENSO, however, as La Nina storms form farther to the south in the Gulf region, resulting in landfalls along the Central American coastline and positive La Nina landfall count anomalies for the Central America Gulf category. El Nino

storms form farther to the north near the US Gulf coast, thus leading to positive El Nino landfall count anomalies for the US Gulf category. Both of these results support the findings that El Nino phase increases the fraction of storms to make landfall along the US coast and La Nina phase favors the Central American and Canadian coasts as mentioned earlier.

Neuron 4 has a very small number of storms (3), thus there are no significant component 1 or component 2 anomalies, and any contributions made to the influence of ENSO on landfall counts are relatively small.

Neuron 5 has two distinct and relatively strong centers of high pressure, one over the central Atlantic and one over the Great Lakes region of the US with a weakness along the east coast of the US. 7 of the 11 storms in this neuron make landfall during La Nina months. Positive component 1 is present for the US Atlantic and Central America Gulf categories. Of the storms that form in the Atlantic, a positive El Nino landfall count anomaly (component 2) exists for the US Atlantic category while a positive La Nina landfall count anomaly is present for the Canada Atlantic category. This indicates that during El Nino phase within this synoptic pattern, storms that form in the Atlantic recurve farther to the west and make landfall along the US coast as compared to their La Nina phase counterparts which make landfall along the Canadian coast.

Neuron 6 synoptic pattern is very similar to that of neuron 5 with the primary difference being that both centers of high pressure are weaker. In addition, storm formation is noticeably favored over the Gulf region as compared to the Atlantic. This supports the positive component 1 for the Central America Gulf category. Positive La Nina landfall count anomalies are present for this category as well, while positive El Nino landfall count anomalies exist for the US Gulf category. Origin location is the primary factor in this dichotomy as storms that form in the Gulf during the El Nino phase form farther north in the region near the US Gulf coast whereas storms that form in La Nina phase form farther to the south near the coast of Central America. For the storms that form in the Atlantic, positive La Nina landfall count anomalies are present for

both Central America and for Canada. These anomalies indicate that storms that form in the Atlantic during La Nina phase either maintain a westward trajectory along the southern periphery of both centers of high pressure and make landfall along the Central American coastline or recurve through the weakness between the ridges and make landfall along the Canadian coastline. This supports the regression analysis results shown in Table 3-1.

Neuron 7 contains only 6 storms, with 5 of the 6 making landfall during La Nina months. The distinguishing feature of the synoptic pattern in this neuron is the presence of a third center of high pressure in the Northern Atlantic just to the northwest of the Iberian Peninsula. There exists no positive component 1 within this neuron, and any landfall count anomalies are relatively modest compared to other neurons.

Neuron 8 contains a large majority (~80%) of landfalls during La Nina months. Two centers of high pressure are present, but comparatively weak. The most westward center of high pressure is even farther west than in neurons 5-7 with the center now located over the Central Great Plains region of the US. Storm origin location is favored to be farther south for this neuron as the vast majority of storms form south of 20 degrees N latitude. As a result, Central America experiences more landfalls in this neuron with positive component 1 present for the Central America Gulf category. In addition, positive La Nina landfall count anomalies are present for both the Central America Atlantic and Gulf categories. For Atlantic storms, a positive La Nina landfall count anomaly exists for the Canada Atlantic category. This neuron, again, illustrates the fact that during La Nina phase with the presence of two centers of high pressure in the studied region, storms that form over the Atlantic either stay far to the south and make landfall along the Central American coastline or recurve through the weakness between the anticyclones and hit the Canadian coastline.

Analysis of the SOM surface pressure maps and associated ENSO phase statistics indicate that both ENSO impact on synoptic pattern frequency and ENSO impact on storm

genesis location, and thus storm advection through a given synoptic pattern, result in a tendency for La Nina storms to avoid the US coast in favor of the coasts of Canada and Central America. For the US, these effects largely counteract the La Nina induced increase in the total number of storms in the Atlantic basin. In contrast, for Canada and Central America, these effects all work in concert to increase the number of landfalls during La Nina months. The left image in Fig. 3-2 illustrates these effects of ENSO on regional landfall patterns (neutral landfalls shown in the right image show no clear favoring of a particular region). Detailed examination of the SOM surface weather maps provides a better physical understanding of the low correlation that exists between ENSO phase and US landfalls shown in Table 3-1.

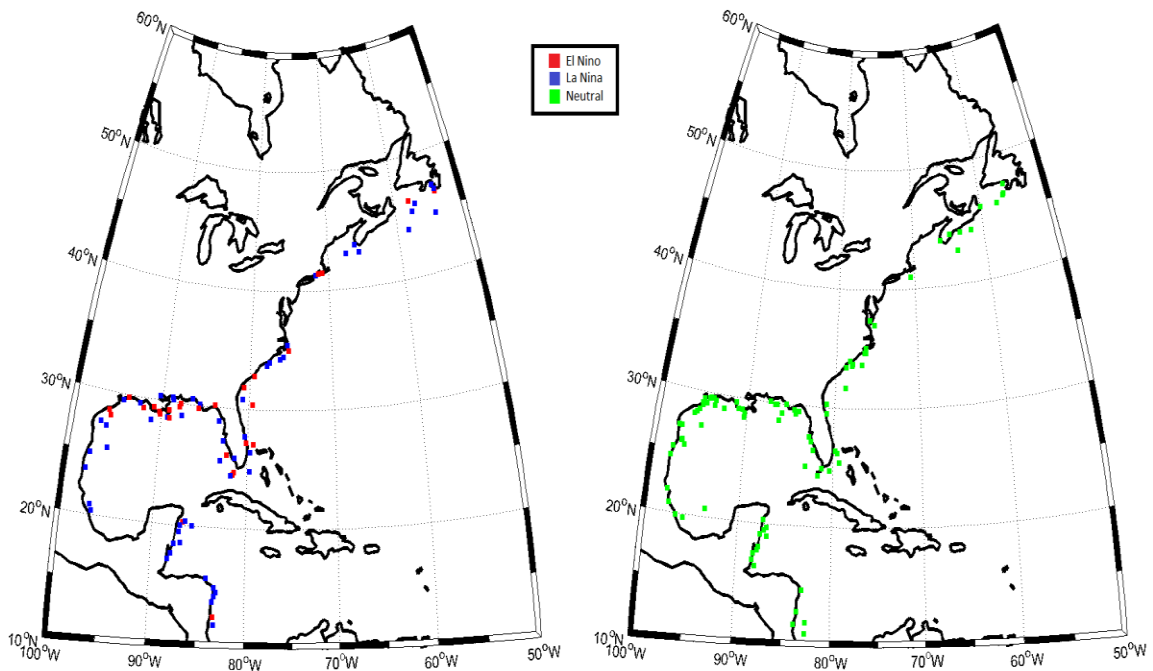


Figure 3-2. Maps of all landfalls along the main coastline of North America. The left map shows all landfalls of tropical cyclones during El Niño months (in red) and La Niña months (in blue). The right map shows all landfalls during neutral months.

Chapter 4

Conclusions

This study investigates the influence of ENSO on seasonal Atlantic basin tropical cyclone landfall count variability within three specified regions of North America – Canada, Central America, and the United States (i.e., US). The study investigated all storms of at least tropical depression strength that formed within the temporal bounds of the hurricane season (1 June – 30 November) over the 33-year period from 1979-2011. Through the use of linear regression analysis, seasonal tropical cyclone counts as well as tropical cyclone landfall counts were determined to be negatively correlated with the sign of ENSO phase (specified by seasonally-averaged ONI values), complimenting many previous studies that have produced these findings. In contrast, landfall counts over the US coastline were shown to lack correlation with, thus be rather insensitive to, the phase of ENSO. This lack of correlation was independent of storm origin location (i.e., Gulf or Atlantic).

The low sensitivity of US landfalls to ENSO phase was further investigated using SOM cluster analysis that determined the predominant synoptic-scale mean sea level pressure patterns present at the time of tropical cyclone landfall. Each cluster (neuron) was considered individually to determine the predominant ENSO phase at the time at which each neuron's storms made landfall. Neurons containing many storms that made landfall during months in which ONI was positive (El Nino) had stronger and larger subtropical ridges centered over the North Atlantic. Moreover these ridges extended farther westward than in neurons containing mostly La Nina neurons. Neurons containing mostly storms that made landfall during La Nina months had two distinct centers of high pressure separated by a weakness.

El Nino conditions induce pressure patterns and affect genesis locations which favor storms to be steered westward along the southern periphery of the comparatively stronger and larger subtropical ridge, eventually recurving into the Gulf of Mexico and making landfall along the Gulf coast of the US. La Nina conditions induce pressure patterns and affect genesis locations which favor storms to be steered either northward through the weakness between the two centers of high pressure, favoring landfalls along the northeastern US and Canadian coastline, or westward to the south of both centers of high pressure, favoring landfalls along the east coast of Central America.

These ENSO-induced changes in synoptic patterns and tropical cyclone tracks provide the insight needed to explain the lack of correlation between US landfall counts and the phase of ENSO. Although El Nino events typically lead to fewer storms in a given hurricane season, those that do form are more likely to make landfall along the Gulf coast of the US. In addition, while La Nina events favor more storms to form in a given hurricane season, they tend to have more scattered landfall distributions over the coast of North America as a result of two distinct centers of high pressure. In La Nina months, storms are more likely to recurve to the east of the US coastline and make landfall in Canada or track westward, remaining south of the US and make landfall along the coast of Central America.

This study was limited to the effects of ENSO on synoptic-scale pressure patterns and these pressure patterns' influence on tropical cyclone tracks/landfall distributions. In addition, the study was confined to the 33-year period of 1979-2011, providing a smaller sample size compared to studies that provide analysis back through the early 1900's. The choice was dictated by the availability of accurate satellite track information.

Further investigation into other teleconnection patterns (e.g., QBO, NAO, AMM, etc.) and their influence on synoptic-scale patterns and tropical cyclone landfall patterns could potentially provide additional understanding of the interannual variability in regional-scale

tropical cyclone landfall counts. A logical next step in this investigation is the creation of a seasonal tropical cyclone landfall count prediction model evaluated for different regions in North America.

These findings illustrate the potential value of a more regional perspective in seasonal tropical cyclone forecasts and, thus, the communication of the potential consequences of these impacts at a regional level. A better understanding of these regional effects can assist in better informing the public, determining appropriate annual preparation activities, and potentially limiting socioeconomic losses.

References

- Bove, M. C., J. J. O'Brien, J.B. Elsner, C.W. Landsea, and X. Niu, 1998: Effect of El Nino on U.S. landfalling hurricanes, revisited. *Bull. Amer. Meteor. Soc.*, 79, 2477-2482.
- Colbert, A. J., and B. J. Soden, 2012: Climatological variations in North Atlantic tropical cyclone tracks. *J. Climate*, 25, 657–673.
- Elsner, J. B., 2003. Tracking hurricanes. *Bull. Amer. Meteor. Soc.*, 84, 353-356.
- Elsner, J. B., and T. H. Jagger, 2004: A hierarchical Bayesian approach to seasonal hurricane modeling. *J. Climate*, 17, 2813–2827.
- Goldenberg, S. B., and L. J. Shapiro, 1996: Physical mechanisms for the association of El Nino and West African rainfall with Atlantic major hurricane activity. *J. Climate*, 9, 1169–1187.
- Gray, W. M., 1984a: Atlantic seasonal hurricane frequency. Part I: El Nino and 30 mb Quasi-Biennial Oscillation influences. *Mon. Wea. Rev.*, 112, 1649–1668.
- Gray, W. M., 1984b: Atlantic seasonal hurricane frequency. Part II: Forecasting its variability. *Mon. Wea. Rev.*, 112, 1669–1683.
- Gray, W. M., C. W. Landsea, P. W. Mielke, and K. J. Berry, 1992: Predicting Atlantic seasonal hurricane activity 6–11 months in advance. *Wea. Forecasting*, 7, 440–455.
- Gray, W. M., C. W. Landsea, P. W. Mielke, and K. J. Berry, 1993: Predicting Atlantic Basin Seasonal Tropical Cyclone Activity by 1 August. *Wea. Forecasting*, 8, 73–86.
- Gray, W. M., C. W. Landsea, P. W. Mielke, and K. J. Berry, 1994: Predicting Atlantic Basin Seasonal Tropical Cyclone Activity by 1 June. *Wea. Forecasting*, 9, 103–115.
- Hart, R. E., and J. L. Evans, 2001: A climatology of extratropical transition of Atlantic tropical cyclones. *J. Climate*, 14, 546-564.

- Hess, J. C., J. B. Elsner, and N. E. LaSeur, 1995: Improving seasonal hurricane predictions for the Atlantic Basin. *Wea. Forecasting*, 10, 425–432.
- Kanamitsu, M., W. Ebisuzaki, J. Woollen, S.-K. Yang, J. J. Hnilo, M. Fiorino, and G. L. Potter, 2002: NCEP–DOE AMIP-II Reanalysis (R-2). *Bull. Amer. Meteor. Soc.*, 83, 1631–1643.
- Kaski, S., 1997: Mathematics, computing, and management in engineering series no. 82. Thesis, Helsinki University of Technology, 57 pp.
- Klotzbach, P. J., 2011: El Niño–Southern Oscillation’s impact on Atlantic Basin hurricanes and U.S. landfalls. *J. Climate*, 24, 1252–1263
- Klotzbach, P. J., 2014: Prediction of Seasonal Atlantic Basin Accumulated Cyclone Energy from 1 July. *Wea. Forecasting*, 29, 115–121.
- Klotzbach, P. J., and W. M. Gray, 2006: Causes of the unusually destructive 2004 Atlantic Basin Hurricane Season. *Bull. Amer. Meteor. Soc.*, 87, 1325–1333.
- Klotzbach, P. J., and W. M. Gray, 2008: Multidecadal Variability in North Atlantic Tropical Cyclone Activity. *J. Climate*, 21, 3929–3935.
- Kohonen, T., 2001: Self-organizing maps. Springer, 511 pp.
- Kossin, J. P., and D. J. Vimont, 2007: A more general framework for understanding Atlantic hurricane variability and trends. *Bull. Amer. Meteor. Soc.*, 88, 1767–1781.
- Kossin, J. P., S. J. Camargo, and M. Sitkowski, 2010: Climate modulation of North Atlantic hurricane tracks. *J. Climate*, 23, 3057–3076.
- Landsea, C. W., W. M. Gray, P. W. Mielke, and K. J. Berry, 1994: Seasonal forecasting of Atlantic hurricane activity. *Weather*, 49, 273–284.
- Lehmiller, G. S., T. B. Kimberlain, and J. B. Elsner, 1997: Seasonal prediction models for North Atlantic basin hurricane location. *Mon. Wea. Rev.*, 125, 1780–1791.
- Pielke, Jr., R. A., and R. A. Pielke Sr., 1997: Hurricanes: Their nature and impacts on society.

Wiley and Sons, 279 pp.

Pielke, Jr., R. A., and C. W. Landsea, 1998: Normalized Hurricane Damages in the United States:

1925-1995. *Wea. Forecasting*, 13, 621-631.

Wilson, R. M., 1999: Statistical aspects of major (intense) hurricanes in the Atlantic Basin during the past 49 hurricane seasons (1950-1998): implications for the current season. *Geophys. Res. Lett.*, 26, 2957–2960.

Yan, T., 2006: Interannual variability of climatology and tropical cyclone tracks in North Atlantic

and Western North Pacific. Dissertation, North Carolina State University, 240 pp.